Heliyon 6 (2020) e05050

Contents lists available at ScienceDirect

Heliyon

journal homepage: www.cell.com/heliyon

Research article

The empirical prediction of weight change and corrosion rate of low-carbon steel

Nurdin Ali [a], Mohamad Ali Fulazzaky [b,c,*]

[a] Department of Mechanical Engineering, Faculty of Engineering, Universitas Syiah Kuala, Jalan Syech Abdurrauf No. 7, Darussalam, Banda Aceh 23111, Indonesia
[b] Environmental Engineering and Management Research Group, Ton Duc Thang University, No. 19, Nguyen Huu Tho Street, Tan Phong Ward, District 7, Ho Chi Minh City 758307, Viet Nam
[c] Faculty of Environment and Labour Safety, Ton Duc Thang University, No. 19, Nguyen Huu Tho Street, Tan Phong Ward, District 7, Ho Chi Minh City 758307, Viet Nam

ARTICLE INFO

Keywords:
Environmental science
Materials science
Corrosion rate
Immersion time
Low-carbon steel
NaCl solution
Weight change

ABSTRACT

Understanding the corrosion rate of metallic building materials is very important to maximize their beneficial use of public facilities. Direct measurements of the weight change and corrosion rate would be time consuming and expensive. This study aims to develop new empirical models based on the experimental data of testing 25 specimens immersed in five different environments for predicting the weight change and corrosion rate of the low-carbon steel. Using the equation developed based on the correlation between corrosion rate and chloride ion concentration is able to predict the corrosion rate of low-carbon steel at the limited chloride ion concentration. An increase in the trend lines of plotting the modeled and measured weight change of low-carbon steel versus immersion time is very similar to each other and progressively increase with increasing of the NaCl concentration. The corrosion rate of low-carbon steel increases from 0.202 to 0.286 mm/y with increasing of the NaCl concentration from 0 to 5% (w/w) in aqueous solution. The weight change and corrosion rate of the steel material are predicted using the new empirical models to contribute to the most reliable applications of low-carbon steel building materials in the future.

1. Introduction

Corrosion is the degradation of the material properties when exposed to an environment such as soil, water and atmosphere resulting in the loss of the material [1, 2, 3]. The most common case of corrosion is the corrosion of metal and steel by water and has the unique characteristics due to the interaction of corrosive material with various anions present in water [4]. The presence of chloride ion (Cl^-) at certain concentrations in water can accelerate the corrosion process during a reasonable time [2, 5] due to a typical ionic compound of sodium chloride (NaCl) can completely dissolve in water to form Na^+ and Cl^- ions and is classified as strong electrolyte [6, 7]. An increase in the concentration of Cl^- ions in water can lead to an increase of the current density, which is proportional to the rate of electrochemical reaction to speed up the corrosion process [8, 9]. The presence of oxygen as a fundamental element for the cathodic process of metallic corrosion in aqueous media can affect the redox reactions during the corrosion process [10].

Low-carbon steel building systems of constructing the various public facilities are a combination of cold-formed steel and welded plate sections forming a structure to place on the Earth's surface or within the water while the steel building costs can be optimized by using the pre-engineered building construction technology [11]. Current uses of low-carbon steel building systems include the manufacturing plants, offices, recreational centers, retail centers, shopping malls, warehouses and many other low-rise building end-uses faced some difficulties and challenges to predict the reliability of lifetime of the steel materials and therefore need some efforts of finding effective ways and providing a theoretical basis for the uses and rapid development of the low-carbon buildings [12]. The electrochemical method of accelerated corrosion reveals a limiting stage of the metal degradation and can be suggested for use in the prediction of corrosion rate [13]. To understand the weight change and corrosion rate of the low-carbon steel requires an understanding of corrosive material immersed in different environments by modeling the experimental data. A scientific knowledge is needed towards the technical goals of being able to predict the loss of corrosive material in an environment and to estimate the lifetime of low-carbon steel structure.

* Corresponding author.
E-mail address: mohamad.ali.fulazzaky@tdtu.edu.vn (M.A. Fulazzaky).

https://doi.org/10.1016/j.heliyon.2020.e05050
Received 3 December 2019; Received in revised form 23 February 2020; Accepted 21 September 2020

A number of studies have been conducted to investigate the corrosion behaviors of the corrosive materials. The corrosion inhibition performance and anticorrosive properties of Hexa (3-methoxy propan-1,2 diol) cyclotriphosphazene on the carbon steel have been investigated by the measurement of the weight loss [14]. Effect of the NaCl concentration on the corrosion rate of carbon steel has been studied in the CO_2 environment [15]. The corrosion rate of the micro-alloyed steels has been determined using the aerated and de-aerated brine solutions [16]. Influence of the water salinity on the structural steel specimens has been investigated along the Gdansk Bay of Poland [17]. Effect of the NaCl concentration on the wear-corrosion behavior of SAF 2507 alloys has been assessed to get better understanding on the tribocorrosion behavior of the alloys employed in corrosive environment with the different phases [18]. The influences of phosphate content and CO_2 have been investigated to control the carbon steel corrosion by vegetable polyol phosphate [19]. Even though many theoretical and empirical models have been developed to describe the atmospheric and water corrosion behaviors of the metals [20, 21, 22], the development of the empirical models for the prediction of the weight change and corrosion rate of the corrosive materials caused by electrochemical oxidation of Cl^- ions in the concentrated solutions is still not fully understood.

The objectives of this study are: (1) to conduct the experiments by immersing the low-carbon steel specimens into five different NaCl concentrations of 0, 2, 3, 4 and 5% (w/w) during the experimental period of 75 days, (2) to create the linear equation by plotting the bilogarithmic graph of weight change versus time based on the experimental data of monitoring 25 specimens and then to develop the new empirical models for the prediction of weight change and (3) to test the validity of empirical prediction of the weight change for convincing the use of the new empirical models to predict the corrosion rate of low-carbon steel at the limited NaCl concentrations in aqueous solution.

2. Materials and methods

2.1. Materials

This study used one low-carbon steel plate of metallic material originally purchased from a steel shop in Banda Aceh city of Indonesia. The steel plate was then cut to have a cross-section specimen with its dimension of 80-mm length, 24-mm width and 3-mm thickness. Approximately 30 cross-section specimens were produced from one steel plate to serve as the samples and controls during the running of the experiment. Approximately 3 kg of the NaCl crystals with a high purity grade in the range of 98.0–99.9% originally purchased from PT. Garam (Persero) in Banda Aceh was used in the preparation of the aqueous salt solutions.

2.2. Mechanical properties and chemical composition

The mechanical properties of the low-carbon steel were tested using the GOTECH testing machines Inc., at the Laboratory of Department of Materials and Design Engineering, Universiti Tun Hussein Onn Malaysia, according to the ASTM E8/E8M-13 Standard Test Method for tension testing of metallic materials. The chemical composition of the low-carbon steel was analyzed using the High Grade PDA-7000 Optical Emissions Spectrometer (Shimadzu Corporation, Kyoto, Japan). The microstructure image of the low-carbon steel was scanned using the Metallurgical Microscope Olympus GX51 (Microscope Systems Limited, Glasgow, UK).

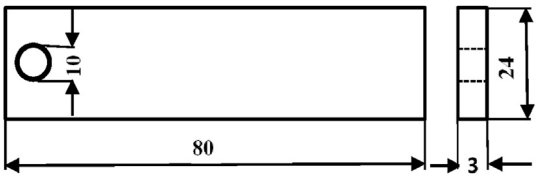

Fig. ure 1Shape and size of the sample (in mm).

2.3. Sample preparation and experimental procedure

This study used 25 cross-section specimens to run an experiment for the collection of data for the development of the new empirical models to predict the weight change and corrosion rate of the low-carbon steel. Each cross-section specimen of the low-carbon steel was fixed a hole of 10-mm diameter as shown in Figure 1 and polished using the silicon carbide abrasive paper with a grit range of P180 to P800. The polished low-carbon steel specimens were then washed with water, cleaned with ethyl alcohol and dried at room temperature. Then each specimen of the low-carbon steel was weighed to have a set of data at most three-decimal place accuracy. Of the 25 specimens were then divided into 5 different treatment groups. 5 specimens of first group (or control specimens) were immersed in distilled water. 5 specimens of second group were immersed in 2% (w/w) NaCl solution. 5 specimens of third group were immersed in 3% (w/w) NaCl solution. 5 specimens of fourth group were immersed in 4% (w/w) NaCl solution. 5 specimens of fifth group were immersed in 5% (w/w) NaCl solution.

Corrosion testing of the first, second, third, fourth and fifth group specimens was carried out by immersing them into the solutions contained of 0, 2, 3, 4 and 5% (w/w) NaCl, respectively, during the experimental period of 1800 h (75 d). A continuous supply of compressed air was carried out during the immersion process to ensure the NaCl solutions contained sufficient oxygen as a precondition of the corrosion process of steel progresses [23, 24]. Each specimen of low-carbon steel immersed in the NaCl solution with a pH of 7.2 was left at room temperature. The monitoring of the low-carbon steel weight change in a salty environment was carried out 7 times with the observation intervals of 240, 480, 720, 960, 1200, 1440 and 1750 h. The effects of immersion time and NaCl concentration on the weight change of low-carbon steel were investigated to gain an accurate and deep understanding of the experimental data for use in the development of the empirical models.

2.4. Determination of the weight change and corrosion rate

The cross sectional area of each low-carbon steel specimen was calculated using the equation [25] of:

$$A = 2\,[(LW) + (LH) + (WH)] \quad (1)$$

where A is the cross sectional area of the low-carbon steel specimen (in mm^2), L is the length of the low-carbon steel specimen (in mm), W is the width of the low-carbon steel specimen (in mm) and H is the thickness of the low-carbon steel specimen (in mm).

In this work, the weight change of low-carbon steel can be obtained by monitoring a change in the weight of specimen during the experiment and by calculating a change in the weight of specimen using the empirical model. The weight change of low-carbon steel occurred by immersing each specimen in the NaCl solution was determined according to ASTM

Table 1. Mechanical properties of the low-carbon steel specimen.

Ultimate tensile strength (MPa)	Yield strength (MPa)	Elongation (%)	Young modulus (GPa)
502	359	32.3	18.87

Table 2. Chemical composition of the low-carbon steel specimen.

C (%)	Si (%)	Mn (%)	P (%)	S (%)	Ni (%)	Cr (%)	Al (%)	Fe (%)
0.231	0.201	0.433	0.006	0.021	0.042	0.023	0.021	Balance

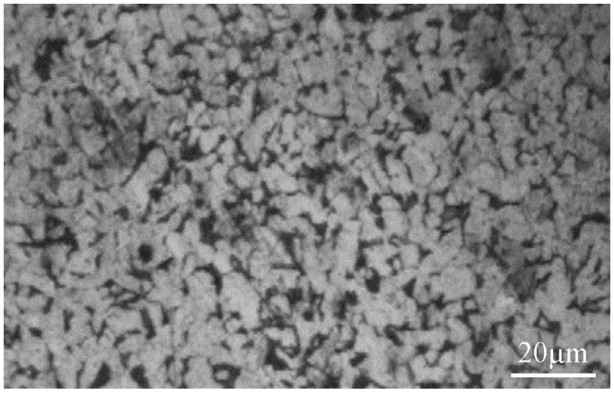

Figure 2. Microstructure image of the low-carbon steel etching with Nital at 5% by weight (alcohol solution of nitric acid) with a magnification of 100 times.

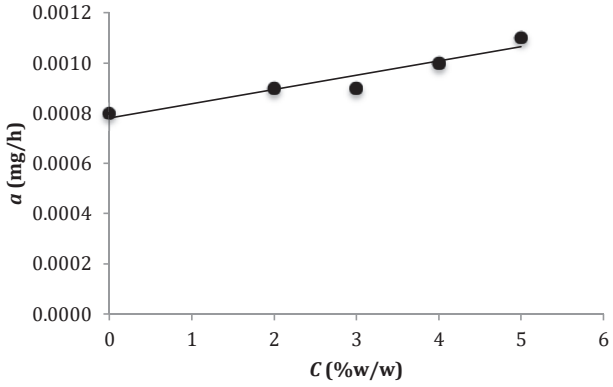

Figure 4. Curve of plotting a versus C.

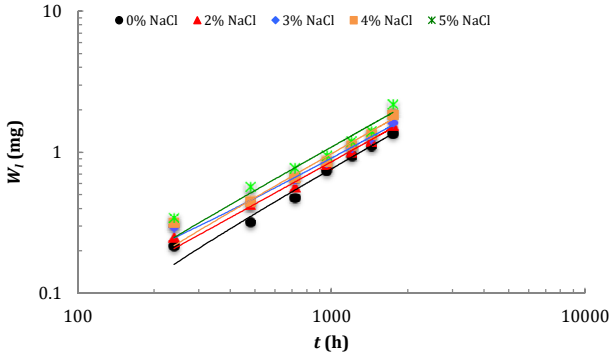

Figure 3. Curves of plotting ln (W_L) versus ln(t) for different low-carbon steel specimens.

G31-72 [26]. One of the main goals of this study was to develop an empirical model that probably matches the experimental data. The use of the empirical model established by plotting the weight change of low-carbon steel against the immersion time was able to predict a theoretical weight change of the low-carbon steel. A quantitative analytical method was used to calculate the corrosion rate of each specimen based on the predicted weight change of low-carbon steel. The corrosion rate of specimen can be calculated using the equation [27] of:

$$C_r = \frac{87.6 W_L}{A t \rho} \quad (2)$$

where C_r is the corrosion rate of the low-carbon steel specimen (in mm/y), W_L is the weight change of the low-carbon steel specimen (in mg) and t is the immersion time (in h), ρ is the density of the low-carbon steel specimen (in g/cm^3).

By plotting the average C_r value versus the NaCl concentration (C) this can provide a theoretical insight into the calculation methodology of using the new empirical model to calculate the corrosion rate of low-carbon steel based on the concentration of chloride ions in the aqueous solution.

3. Results and discussion

3.1. Image of the low-carbon steel microstructure

The mechanical properties (see Table 1) of the low-carbon steel are relatively soft and weak but have outstanding ductility and toughness as shown by an ultimate tensile strength of 502 MPa, yield strength of 359 Mpa, elongation of 32.3% and young modulus of 18.87 Gpa [28, 29]. The chemical composition of the metal plate material with an average C content of 0.231% (see Table 2) indicates that the cross-section specimen used in this study is the low-carbon steel or mild steel. Low-carbon steel has no dominant element in spite of the average Mn content of 0.433% is higher than the average C content of 0.231%. A microstructure image of Figure 2 shows that the light and dark areas observed on the surface of low-carbon steel specimen correspond to ferrite and fine pearlite, respectively [30]. The microstructure of low-carbon steel consisting of light and dark grains with their sizes of relatively uniform corresponds to proeutectoid ferrite and colonies of pearlite, respectively [31]. The appearance of long sub-critical annealing on the surface of low-carbon

Table 3. Values of the parameters a, b in the equation: ln (W_L) = a ln(t) + b.

NaCl concentration (%w/w)	a (mg/h)	b (mg)	R^2
0	0.0008	- 0.0292	0.99149
2	0.0009	0.0035	0.99265
3	0.0009	0.0389	0.99366
4	0.0010	- 0.0209	0.97662
5	0.0011	- 0.0158	0.94117

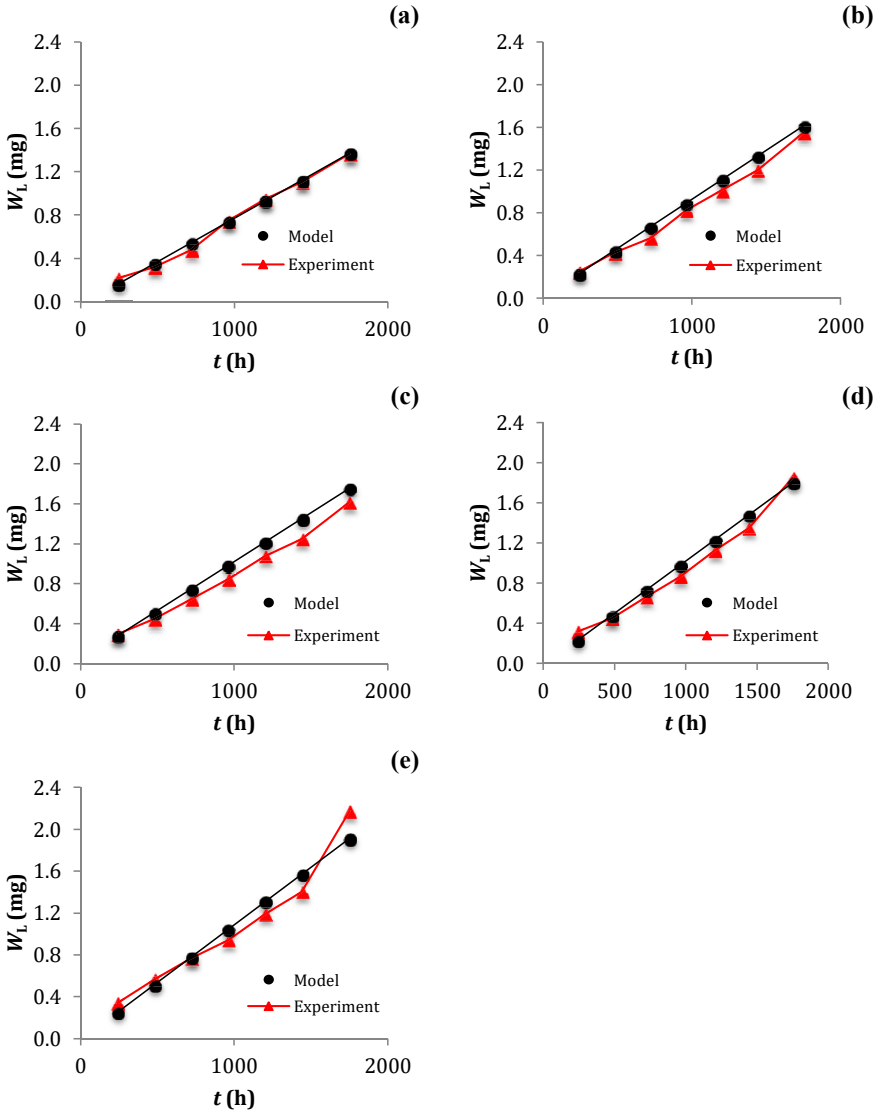

Figure 5. Curves of plotting W_L versus t with (a) 0% (w/w) NaCl in solution, (b) 2% (w/w) NaCl in solution, (c) 3% (w/w) NaCl in solution, (d) 4% (w/w) NaCl in solution and (e) 5% (w/w) NaCl in solution.

Table 4. Weight change of the low-carbon steel pursuant to the immersion time.

t (h)	W_L (mg)									
	0% NaCl		2% NaCl		3% NaCl		4% NaCl		5% NaCl	
	Model	Exp.	Model	Exp.	Model	Exp.	Model	Exp.	Model	Exp.
240	0.163	0.216	0.224	0.248	0.274	0.293	0.229	0.318	0.248	0.343
480	0.355	0.320	0.445	0.426	0.509	0.446	0.478	0.449	0.512	0.569
720	0.547	0.475	0.666	0.563	0.745	0.646	0.728	0.662	0.776	0.766
960	0.739	0.746	0.887	0.822	0.980	0.847	0.978	0.865	1.040	0.942
1200	0.931	0.945	1.108	1.007	1.215	1.079	1.227	1.121	1.304	1.191
1440	1.123	1.105	1.328	1.197	1.450	1.248	1.477	1.347	1.568	1.402
1750	1.371	1.364	1.614	1.550	1.754	1.617	1.799	1.854	1.909	2.171

steel may be related to a redistribution of the cementite in form of the pseudo-spherical pearlite agglomerates [32].

3.2. Weight change

The weight change of cross-section specimen as an indicator for monitoring the corrosion rate of metallic material can be calculated based on the difference of initial weight before immersion to actual weight of the low-carbon steel specimen after immersion in the NaCl solution [33]. By measuring the weight change of low-carbon steel per unit of surface per unit of time permits us to determine the corrosion rate of low-carbon steel immersed in a series of solution of different NaCl concentrations according to Eq. (2). Even though the bilogarithmic model has been proposed for the long-term prediction of the metal

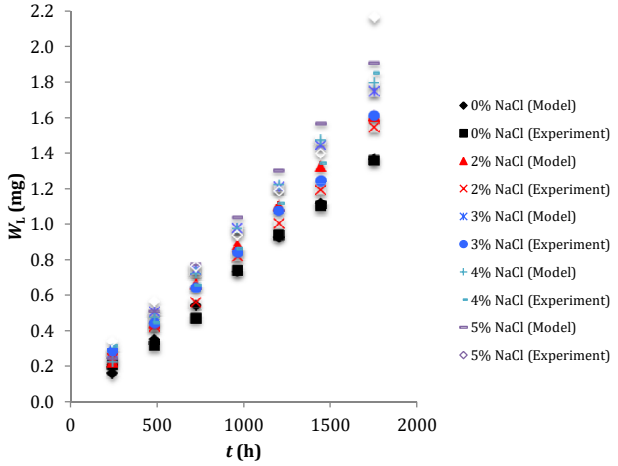

Figure 6. Results of plotting W_L versus t according to the calculated data using Eq. (5) and the experimental data.

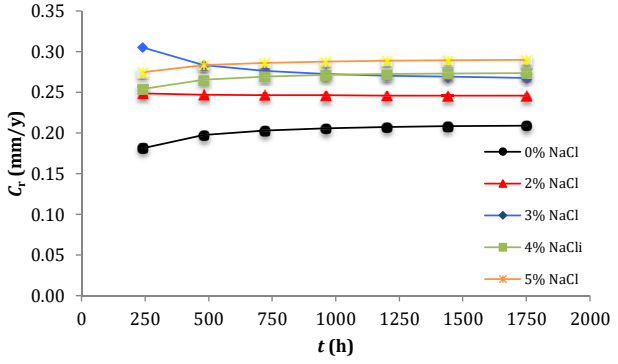

Figure 7. Curves of plotting C_r versus t for different NaCl concentrations in the solution.

corrosion mass losses in the atmosphere [34], the application of a new bilogarithmic model developed to predict the weight change of low-carbon steel immersed in aqueous solution must be verified. A plot (Figure 3) of ln (W_L) versus ln(t) yields the curves all fitting with a linear model where a is the slope of the linear regression line and b is the W_L-intercept. Correlation for the parameters a, b in the curves is very good with R^2 is higher than 0.9411 (see Table 3). An equation of modeling the graphs in Figure 3 can be expressed in the linear form [35, 36] of:

$$\ln(W_L) = a \ln(t) + b \,, \tag{3}$$

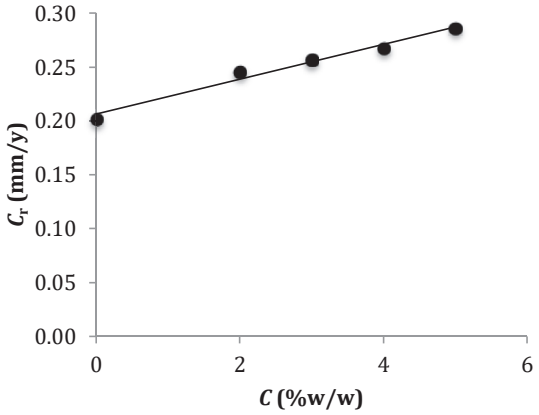

Figure 8. Curve of plotting C_r versus C for predicting the corrosion rate at a limited NaCl concentration in the solution.

where W_L is the weight change of the low-carbon steel (in mg), t is the immersion time (in h), a is the correlation coefficient (in mg/h) and b is the constant relating to the solution environments (in mg).

The weight change of the metallic material affected by the electrochemical process with the application of the treated *Rhizopora mucronata* tannin and *Luffa cylindrica* leaf extract as the corrosion inhibitors to protect the low-carbon steel increases with increasing of the NaCl concentration in the solution [37, 38]. Empirical evidence (Table 3) shows that the value of a increased from 0.0008 to 0.0011 mg/h with increasing of the NaCl concentration in solution from 0 to 5% (w/w) could be due to the passive layer on low-carbon steel is susceptible to chloride attacks [2]. By plotting a versus C as shown in Figure 4 yields a very strong relationship of the linear regression line with the R^2 value of 0.91684 and can be expressed in the linear equation as:

$$a = 0.00006\, C + 0.0008 \,, \tag{4}$$

with C is the NaCl concentration in solution (in %w/w).

The substitution of Eq. (4) into Eq. (3) makes it possible to remove a logarithm from an equation and yields a new equation of:

$$W_L = (0.00006\, C + 0.0008)\, t + b \,, \tag{5}$$

Even though several empirical models developed for testing the corrosion data that having their typical curves could be useful to formulate an equation of generalizing the experimental findings [39, 40, 41], this study is limited to develop a new empirical equation with typical use in the prediction of the weight change of low-carbon steel immersed in the saline solution over time. Using Eq. (5) permits us to calculate the weight change of low-carbon steel at any time of low-carbon steel specimen immersed in saline solution since the values of b and C have been verified from the linear curve. The validation (Figure 5, see Table 4) of the new empirical model shows that the trend lines of plotting the theoretical data calculated using Eq. (5) are almost similar to those of

Table 5. Corrosion rate of the low-carbon steel pursuant to the immersion time.

t (h)	C_r (mm/y)				
	0% NaCl	2% NaCl	3% NaCl	4% NaCl	5% NaCl
240	0.181	0.249	0.305	0.254	0.274
480	0.197	0.247	0.283	0.265	0.283
720	0.203	0.246	0.276	0.269	0.286
960	0.205	0.246	0.273	0.271	0.288
1200	0.207	0.246	0.270	0.272	0.289
1440	0.208	0.246	0.269	0.273	0.289
1750	0.209	0.246	0.268	0.274	0.290

plotting the experimental data measured during the experiment. The average errors of 1.08%, 7.31%, 10.84%, 4.33% and 0.35% were verified for the cross-section specimens of low-carbon steel immersed in the solutions of containing 0%, 2%, 3%, 4% and 5% (w/w) of the NaCl concentration, respectively. A decrease in the average error from 10.84 to 7.31 to 4.33 to 1.08 and to 0.35% for a change in the composition of solution from 3% to 2%–4% to 0% and to 5% (w/w) of the NaCl concentration, respectively, could be due to a perturbed composition of the NaCl solution affected Cl^- mobilization can attack the surface layer of low-carbon steel used to monitor the pitting corrosion of cross-section specimen [2, 42, 43]. Many factors can affect the corrosion behaviors of low-carbon steel immersed in saline solution. The formation of rust according to the chemical equation: $4\ Fe(s) + 3\ O_2(g) \rightarrow 2\ Fe_2O_3(s)$ may accelerate the corrosion process of low-carbon steel [44] and makes it possible to interfere the mobilization of Cl^- ions towards the surface of cross-section specimen. Despite this study didn't consider the solubility of oxygen as function of NaCl concentration, the effect of NaCl concentration on the solubility of oxygen has been previously investigated to gain better understanding on the corrosion behavior of proprietary micro-alloyed steels in brine solutions [16].

The results (Figure 6) of plotting W_L versus t show the weight change of low-carbon steel gradually increased with increasing of the immersion time and progressively increased with increasing of the NaCl concentration. Using Eq. (5) permits us to predict the change of low-carbon steel in an aqueous environment and may simulate any environmental condition to which a weight change level of the mild steel structure may occur in the saline water at any time. It has been reported that the immersion time and the level of dissolved oxygen (DO) in aqueous solution can influence the morphology and composition of the corrosion products formed on the low-carbon steel in NaCl solution [45]. Effect of Cl^- ions on the weight change of low-carbon steel can be interpreted by the characterization of the metal complexes formed between Fe contained in mild steel and the Cl^- ions [46]. An increase in the weight change of E-34 microalloyed steel could be due to an increased NaCl concentration in the solution [47]. The presence of such as Mg^{2+} ions as a splicing inhibitor element in saline solution can lower the electron transfer of corrosion rust layer on the Cr-containing steel [48]. The formation of calcium alginate composite barrier layer on the defect region of low-carbon steel has a good adhesion capability in the protection of corrosion for the water-delivery pipelines [49]. The surface modification by the implantation of nitrogen ion can increase the corrosion resistance of commercially pure titanium [50].

3.3. Corrosion rate

The corrosion rate of low-carbon steel as a consequence of the chemical action is an important parameter of the corrosion and may govern the generation of sites for arsenic removal in the treatment of water [51]. The destructive and unintentional attack of low-carbon steel may occur on the surface of cross-section specimen immersed in the NaCl solution. Using Eq. (1) permits us to calculate the cross sectional area of low-carbon steel specimen. Using Eq. (2) permits us to calculate the corrosion rate of low-carbon steel based on the value of W_L theoretically calculated using Eq. (5). By plotting the curve of C_r versus t (see Figure 7) shows that the corrosion rate of low-carbon steel, except for 3% NaCl in the solution, increases with increasing of the NaCl concentration and is almost constant after exposure for 720 h of the immersion. This contradicts the findings of determining the instantaneous corrosion rate of C1018 carbon steel in CO_2-saturated solutions by the electrochemical impedance spectroscopy and linear polarization resistance that the corrosion rate of C1018 carbon steel decreases with increasing of the NaCl concentration [15]. A decrease in the corrosion rate of low-carbon steel immersed in the NaCl solution could be due to a decrease in the DO and HCO_3^- concentrations or an increase in the immersion time [45]. Empirical prediction (see Table 5) of mild steel degradation rate at 1750 h of the immersion time increases from 0.209 to 0.246 to 0.268 to 0.274 and to 0.290 mm/y with increasing of the NaCl concentration from 0 to 2 to 3 to 4 and to 5% (w/w), respectively. An increase in the NaCl concentration is capable of donating more free Cl^- ions to the solution and leads to a failure of the mild steel caused by the surface deterioration and presence of the micro/macro-pits [52]. The corrosion rate can be influenced by the presence of settled bacteria in the biofilm and by the immersion time [53]. The top of line corrosion rate of low-carbon steel affected by mono ethylene glycol in acetic acid may occur at elevated temperature environment [54]. The presence of Cl^- ions can attack the passive layer to diffuse into the local corrosion sites and catalyze the corrosion process thereby promoting further corrosion [55, 56].

Both the anodic and cathodic reactions take place during the corrosion process. In the anodic reaction, Fe^{2+} ions pass into solution leaving their electrons within the surface of original low-carbon steel. In the cathodic reaction, the free electrons within the surface of original low-carbon steel are gained by the chemical species of O_2 and H_2O for use in the reduction reaction. It is possible to calculate the corrosion rates of low-carbon steel caused by different corrosion currents generated from different concentrations of NaCl in the solution. By plotting C_r versus C (see Figure 8) yields a straight line with a very strong relationship ($R^2 = 0.978$) and can be written in the equation form of:

$$C_r = 0.0162\ C + 0.2064\ . \tag{6}$$

Using Eq. (6) permits us to predict the corrosion rate of low-carbon steel when the specimen of low-carbon steel is immersed into different concentrations of NaCl in the solution. Empirical evidence (Figure 8) shows that the average value of C_r linearly increases from 0.202 to 0.246 to 0.257 to 0.268 and to 0.286 mm/y deals with increasing of the NaCl concentration from 0 to 2 to 3 to 4 and to 5% (w/w). The stressed induced surface chemistry is an important aspect of stress-corrosion cracking when the specimen of low-carbon steel is immersed in the NaCl solution [57]. For the infrastructure applications in a marine environment, the corrosion damage of mild steel is likely to increase with increasing of the NaCl concentration [40, 43]. The establishment of the new equation: $C_r = 0.0162\ C + 0.2064$ may contribute to the prediction of corrosion rate at a limited NaCl concentration in solution for the applications of low-carbon steel to private and public infrastructures in the future. The lifetime of low-carbon steel specimen immersed in the saline water can be predicted using Eq. (6) to allow the prediction of low-carbon steel structure age since the concentration of NaCl in solution has been verified as a key factor for salt stress tolerance of the mild steel structure degradation in an aqueous environment.

4. Conclusions

The new empirical models was developed based on the experimental data of testing 25 cross-section specimens immersed in five different NaCl concentrations and can be used for the prediction of the weight change and corrosion rate of the low-carbon steel. Using the equation: $W_L = (0.00006\ C + 0.0008)\ t + b$ permits us to predict the weight change of low-carbon steel as function of the exposure time. Using the equation: $C_r = 0.0162\ C + 0.2064$ permits us to predict the corrosion rate of low-carbon steel at a limited NaCl concentration in solution. The validation of these empirical models showed a very strong relationship with the R^2 values of higher than 0.9168. The result findings contribute to an investigation of the usability of low-carbon steel structures in the future.

Declarations

Author contribution statement

Nurdin Ali: Conceived and designed the experiments; Performed the experiments; Analyzed and interpreted the data; Contributed reagents, materials, analysis tools or data; Wrote the paper.

Mohamad Ali Fulazzaky: Conceived and designed the experiments; Analyzed and interpreted the data; Wrote the paper.

Funding statement

This work was supported by Universitas Syiah Kuala, Indonesia (Research Grant Scheme No. 289/UN11/PSP/PNBP/2018) and Ton Duc Thang University, Vietnam (Contract No. 551/2019/TĐT-HĐLV-NCV).

Competing interest statement

The authors declare no conflict of interest.

Additional information

The raw/processed data required to reproduce these findings cannot be shared at this time due to legal or ethical reasons. The raw/processed data required to reproduce these findings cannot be shared at this time as the data also forms part of an ongoing study.

References

[1] E.S.M. Sherif, Comparative study on the inhibition of iron corrosion in aerated stagnant 3.5 wt% sodium chloride solutions by 5-phenyl-1H-tetrazole and 3-amino-1,2,4-triazole, Ind. Eng. Chem. Res. 52 (2013) 14507–14513.
[2] Y. Song, G. Jiang, Y. Chen, P. Zhao, Y. Tian, Effects of chloride ions on corrosion of ductile iron and carbon steel in soil environments, Sci. Rep. 7 (2017) 6865.
[3] Y. Yan, A. Neville, D. Dowson, Understanding the role of corrosion in the degradation of metal-on-metal implants, Proc. Inst. Mech. Eng. H 220 (2006) 173–181.
[4] G.S. Frankel, J.D. Vienna, J. Lian, J.R. Scully, S. Gin, J.V. Ryan, J. Wang, S.H. Kim, W. Windl, J. Du, A comparative review of the aqueous corrosion of glasses, crystalline ceramics, and metals, NPJ Mater. Degrad. 2 (2018) 15.
[5] L.A. Bromley, Thermodynamic properties of strong electrolytes in aqueous solutions, AIChE J. 19 (1973) 313–320.
[6] A.A. Dastgerdi, A. Brenna, M. Ormellese, M. Pedeferri, F. Bolzoni, Electrochemical methods for the determination of Pedeferri's diagram of stainless steel in chloride containing environment, Mater. Corros. 70 (2019) 9–18.
[7] R.K. Kalluri, T.A. Ho, J. Biener, M.M. Biener, A. Striolo, Partition and structure of aqueous NaCl and $CaCl_2$ electrolytes in carbon-slit electrodes, J. Phys. Chem. C 117 (2013) 13609–13619.
[8] L. Bazinet, D. Ippersiel, C. Gendron, B. Mahdavi, J. Amiot, F. Lamarche, Effect of added salt and increase in ionic strength on skim milk electroacidification performances, J. Dairy Res. 68 (2001) 237–250.
[9] J. Chen, Z. Chen, Y. Ai, J. Xiao, D. Pan, W. Li, Z. Huang, Y. Wang, Impact of soil composition and electrochemistry on corrosion of rock-cut slope nets along railway lines in China, Sci. Rep. 5 (2015) 14939.
[10] L.T. Popoola, A.S. Grema, G.K. Latinwo, B. Gutti, A.S. Balogun, Corrosion problems during oil and gas production and its mitigation, Int. J. Ind. Chem. 4 (2013) 35.
[11] M.U. Saleem, H.J. Qureshi, Design solutions for sustainable construction of pre-engineered steel buildings, Sustainability 10 (2018) 1761.
[12] J. Tang, X. Cai, H. Li, Study on development of low-carbon building based on LCA, Energy Proc. 5 (2011) 708–712.
[13] V.A. Grachev, A.E. Rozen, Y.P. Perelygin, S.Y. Kireev, I.S. Los', A.A. Rozen, Measuring corrosion rate and protector effectiveness of advanced multilayer metallic materials by newly developed methods, Heliyon 4 (2018), e00731.
[14] O. Dagdag, A. El Harfi, M. El Gouri, Z. Safi, R.T.T. Jalgham, N. Wazzan, C. Verma, E.E. Ebenso, U.P. Kumar, Anticorrosive properties of Hexa (3-methoxy propan-1,2-diol) cyclotri-phosphazene compound for carbon steel in 3% NaCl medium: gravimetric, electrochemical, DFT and Monte Carlo simulation studies, Heliyon 5 (2019), e01340.
[15] Z. Zeng, R. S Lillard, H. Cong, Effect of salt concentration on the corrosion behavior of carbon steel in CO_2 environment, Corrosion 72 (2016) 805–823.
[16] L. Onyeji, G. Kale, Preliminary investigation of the corrosion behavior of proprietary micro-alloyed steels in aerated and deaerated brine solutions, J. Mater. Eng. Perform. 26 (2017) 5741–5752.
[17] K. Zakowski, M. Narozny, M. Szocinski, K. Darowicki, Influence of water salinity on corrosion risk - the case of the southern Baltic Sea coast, Environ. Monit. Assess. 186 (2014) 4871–4879.
[18] G. Han, P. Jiang, J. Wang, F. Yan, Effects of NaCl concentration on wear-corrosion behavior of SAF 2507 super duplex stainless steel, RSC Adv. 6 (2016) 111261–111268.
[19] R.C. da Silva, M. Heinen, G.A. Lorenzi, D.W. Lima, J.H.L. Moura, J.M. de Freitas, E.M.A. Martini, C.L. Petzhold, Carbon steel corrosion controlled by vegetable polyol phosphate, in medium containing chloride and glyoxal: influence of phosphate content and CO_2, Heliyon 5 (2019), e01720.
[20] K. Kreislova, D. Knotkova, The results of 45 years of atmospheric corrosion study in the Czech Republic, Mater 10 (2017) 394.
[21] M. Natesan, S. Selvaraj, T. Manickam, G. Venkatachari, Corrosion behavior of metals and alloys in marine-industrial environment, Sci. Technol. Adv. Mater. 9 (2008), 045002.
[22] E. Shafiei, M. Zeinali, A. Nasiri, H. Charroostaei, M.A. Gholamalian, A brief review on the atmospheric corrosion of mild steel in Iran, Cogent Eng. 1 (2014) 990751.
[23] M. Hagarová, J. Cervová, F. Jaś, Selected types of corrosion degradation of pipelines, Koroze a ochrana materiálu 59 (2015) 30–36.
[24] W. Zhao, T. Zhang, Y. Wang, J. Qiao, Z. Wang, Corrosion failure mechanism of associated gas transmission pipeline, Materials 11 (2018) 1935.
[25] D.G. Ellis, Cross-sectional area measurements for tendon specimens: a comparison of several methods, J. Biomech. 2 (1969) 175–186.
[26] American Society for Testing and Materials (ASTM), Standard Practice for Laboratory Immersion Corrosion Testing of Metals. Annual Book of ASTM Standard. ASTM G31-72, ASTM International, 1999.
[27] L. Khaksar, J. Shirokoff, Effect of elemental sulfur and sulfide on the corrosion behavior of Cr-Mo low alloy steel for tubing and tubular components in oil and gas industry, Materials 10 (2017) 430.
[28] W. Cao, M. Zhang, C. Huang, S. Xiao, H. Dong, Y. Weng, Ultrahigh Charpy impact toughness (~450J) achieved in high strength ferrite/martensite laminated steels, Sci. Rep. 7 (2017) 41459.
[29] J. Wadsworth, Connections: superplasticity, Damascus steels, laminated steels, and carbon dating, J. Min. Met. Mater. Soc. 68 (2016) 3150–3160.
[30] S.W. Thompson, P.R. Howell, Factors influencing ferrite/pearlite banding and origin of large pearlite nodules in a hypoeutectoid plate steel, Mater. Sci. Technol. 8 (1992) 777–784.
[31] N. Ochoa, C. Vega, N. Pébère, J. Lacaze, J.L. Brito, CO_2 corrosion resistance of carbon steel in relation with microstructure changes, Mater. Chem. Phys. 156 (2015) 198–205.
[32] W.C. Chiou Jr., E.A. Carter, Structure and stability of Fe_3C-cementite surfaces from first principles, Surf. Sci. 530 (2003) 88–100.
[33] V.A. Grachev, A.E. Rozen, Y.P. Perelygin, S.Y. Kireev, I.S. Los, A.A. Rozen, Measuring corrosion rate and protector effectiveness of advanced multilayer metallic materials by newly developed methods, Heliyon 4 (2018), e00731.
[34] Y.M. Panchenko, A.I. Marshakov, Long-term prediction of metal corrosion losses in atmosphere using a power-linear function, Corr. Sci. 109 (2016) 217–229.
[35] T.Q. Ansari, J. Luo, S. Shi, Modeling the effect of insoluble corrosion products on pitting corrosion kinetics of metals, NPJ Mater. Degrad. 3 (2019) 28.
[36] M.A. Fulazzaky, Measurement of biochemical oxygen demand of the leachates, Environ. Monit. Assess. 185 (2013) 4721–4734.
[37] A. Agi, R. Junin, M. Rasol, A. Gbadamosi, R. Gunaji, Treated *Rhizophora mucronata* tannin as a corrosion inhibitor in chloride solution, PloS One 13 (2018), e0200595.
[38] O.O. Ogunleye, A.O. Arinkoola, O.A. Eletta, O.O. Agbede, Y.A. Osho, A.F. Morakinyo, J.O. Hamed, Green corrosion inhibition and adsorption characteristics of Luffa cylindrica leaf extract on mild steel in hydrochloric acid environment, Heliyon 6 (2020), e03205.
[39] N. Ali, M.A. Fulazzaky, M.S. Mustapa, M.I. Ghazali, M. Ridha, T. Sujitno, Assessment of fatigue and corrosion fatigue behaviours of the nitrogen ion implanted CpTi, Int. J. Fatig. 61 (2014) 184–190.
[40] R.E. Melchers, A review of trends for corrosion loss and pit depth in longer-term exposures, Corros. Mater. Degrad. 1 (2018) 42–58.
[41] S.S. Rajahram, T.J. Harvey, R.J.K. Wood, Evaluation of a semi-empirical model in predicting erosion-corrosion, Wear 267 (2009) 1883–1893.
[42] S. Sundjono, G. Priyotomo, L. Nuraini, S. Prifiharni, Corrosion behavior of mild steel in seawater from northern coast of Java and southern coast of Bali, Indonesia, J. Eng. Technol. Sci. 49 (2017) 770–784.
[43] J. Tang, J. Li, H. Wang, Y. Wang, G. Chen, In-situ monitoring and analysis of the pitting corrosion of carbon steel by acoustic emission, Appl. Sci. 9 (2019) 706.
[44] J. Alcántara, D. de la Fuente, B. Chico, J. Simancas, I. Díaz, M. Morcillo, Marine atmospheric corrosion of carbon steel: a review, Materials 10 (2017) 406.
[45] G.D. Eyu, G. Will, W. Dekkers, J. MacLeod, Effect of dissolved oxygen and immersion time on the corrosion behaviour of mild steel in bicarbonate/chloride solution, Materials 9 (2016) 748.
[46] R.T. Foley, Role of the chloride ion in iron corrosion, Corrosion 26 (1970) 58–70.
[47] A.H. Seikh, Influence of heat treatment on the corrosion of microalloyed steel in sodium chloride solution, J. Chem. 587514 (2013) 1–7.
[48] S.J. Song, J.G. Kim, Influence of magnesium ions in the seawater environment on the improvement of the corrosion resistance of low-chromium-alloy steel, Materials 11 (2018) 162.
[49] J. Cui, X. Li, Z. Pei, Y. Pei, A long-term stable and environmental friendly self-healing coating with polyaniline/sodium alginate microcapsule structure for corrosion protection of water-delivery pipelines, Chem. Eng. J. 358 (2019) 379–388.
[50] M.A. Fulazzaky, N. Ali, H. Samekto, M.I. Ghazali, Assessment of CpTi surface properties after nitrogen ion implantation with various doses and energies, Metallurg. Mater. Transact. A 43 (2012) 4185–4193.
[51] J.M. Triszcz, A. Porta, F.S. García Einschlag, Effect of operating conditions on iron corrosion rates in zero-valent iron systems for arsenic removal, Chem. Eng. J. 150 (2009) 431–439.
[52] R.T. Loto, Anti-corrosion performance of the synergistic properties of benzenecarbonitrile and 5-bromovanillin on 1018 carbon steel in HCl environment, Sci. Rep. 7 (2017) 17555.
[53] H. Zhang, Y. Tian, J. Wan, P. Zhao, Study of biofilm influenced corrosion on cast iron pipes in reclaimed water, Appl. Surf. Sci. 357 (2015) 236–247.
[54] B. Widyanto, I.G.B.E.S. Wiguna, The effect of mono ethylene glycol on the top of line corrosion rate of low carbon steel in acetic acid and elevated temperature environment, Heliyon 5 (2019), e02006.

[55] B. Jeon, S.K.R.S. Sankaranarayanan, A.C.T. van Duin, S. Ramanathan, Reactive molecular dynamics study of chloride ion interaction with copper oxide surfaces in aqueous media, ACS Appl. Mater. Interfaces 4 (2012) 1225–1232.
[56] K.J. Vetter, F. Gorn, Kinetics of layer formation and corrosion processes of passive iron in acid solutions, Electrochim. Acta 18 (1973) 321–326.
[57] W. Liu, J. Sun, C. Ye, The influence of tensile strain on water adsorbed on Fe (100) surface: surface chemistry aspect of stress corrosion cracking, Appl. Surf. Sci. 481 (2019) 192–199.